J Nanopart Res (2014) 16:2606
DOI 10.1007/s11051-014-2606-9

RESEARCH PAPER

Scalable synthesis and functionalization of cobalt nanoparticles for versatile magnetic separation and metal adsorption

Pipsa Mattila · Hanna Heinonen · Kalle Loimula · Johanna Forsman · Leena-Sisko Johansson · Unto Tapper · Riitta Mahlberg · Hans-Peter Hentze · Ari Auvinen · Jorma Jokiniemi · Roberto Milani

Received: 30 May 2014 / Accepted: 7 August 2014 / Published online: 23 August 2014

Abstract Magnetic cobalt nanoparticles coated with a thin carbon shell were produced by means of a scalable method based on hydrogen reduction synthesis. The presence of oxidized groups on the surface of the carbon shell enabled the reaction with alkoxysilanes bearing amino and thiol reactive functions under mild conditions, and therefore the formation of a thin functional silane layer which holds the potential for further modification in consideration of specific applications, e.g., in the separation and catalysis fields. The magnetic nanoparticles bearing surface thiol groups were also used in metal adsorption tests. These nanoparticles could efficiently adsorb not only gold from a chloride salt aqueous solution, but also several other metals when incubated in a thiocyanate-leached solution obtained from crushed printed circuit boards. The combination of a scalable production method with a simple and versatile surface modification strategy opens up a wide array of potential industrial applications in the fields of separation, sensing, and biomedical devices.

Keywords Carbon-coated magnetic nanoparticles · Cobalt · Surface modification · Metal adsorption

Electronic supplementary material The online version of this article (doi:10.1007/s11051-014-2606-9) contains supplementary material, which is available to authorized users.

P. Mattila · H. Heinonen · K. Loimula · J. Forsman · U. Tapper · R. Mahlberg · H.-P. Hentze · A. Auvinen · J. Jokiniemi (✉) · R. Milani (✉)
VTT Technical Research Centre of Finland, P.O.Box 1000, FI-02044 Tampere, Finland
e-mail: jorma.jokiniemi@vtt.fi

R. Milani
e-mail: roberto.milani@vtt.fi

L.-S. Johansson
Department of Forest Products Technology, School of Chemical Technology, Aalto University, P.O.Box 16400, FI-00076 Aalto, Finland

J. Jokiniemi
Department of Environmental Science, University of Eastern Finland, P.O.Box 1627, FI-70211 Kuopio, Finland

Introduction

Magnetic nanoparticles (MNPs) are increasingly used as adsorbents and carriers of different compounds in a wide range of applications since they can be easily separated and collected from solution with a strong magnet. With the newest developments in nanotechnology, various types of MNPs with large surface area and high number of surface active sites have been synthesized. Aggregation of MNPs is prevented by surface modification, and interactions with the target substances to be bound are ensured by conjugating specific reactive functional groups on the particle surface.

Such MNPs as Fe_3O_4 (magnetite) and γ-Fe_2O_3 (maghemite) have been of great interest due to their super-paramagnetic properties (Villani et al. 2013; Zhang et al. 2013). However, bulk ferrite displays a relatively low saturation magnetization ($M_s \leq 92$ emu/g). Furthermore, after the functionalization of nanosized ferrite particles, the distance between the metal cores increases and magnetic separation efficiency decreases significantly (Sun et al. 2005). In contrast to ferrites, carbon-coated cobalt has a much higher M_s from 141 up to 150 emu/g (Forsman et al. 2013).

Cobalt is known to be an allergen. In order to avoid the release of cobalt from the solid state to the liquid phase and to protect the particle surface from oxidation and thereby from decrease of M_s, cobalt particles can be coated with carbon coatings, which can be further functionalized with binding sites having different degrees of selectivity for specific applications.

MNPs have been widely studied for the preparation of magnetic nanocomposites (Behrens 2011), in the field of nanomedicine for e.g. drug delivery, biomedical diagnostics, and therapeutics (Yan et al. 2013; Jedlovszky-Hajdú et al. 2012; Baldelli Bombelli et al. 2014), and have been extensively employed as supporting media and active sites for catalysts, allowing the easy access of reactants as well as convenient catalyst recovery (Zhu et al. 2010). Recent advances in the area of iron oxide and magnetic core–shell nanoparticles include for instance the development of advanced magnetic resonance imaging and near-infrared agents, also involving novel preparation methods such as microfluidic synthesis (Song et al. 2011; Seo et al. 2006, 2012, 2013).

MNPs have shown great potential also for environmental detection and remediation, where surface-functionalized magnetic adsorbents allow effective sensing and removal of pollutants from water due to their large surface area and small diffusion resistance (Liu et al. 2011). Increasing environmental and health concerns in particular have drawn attention to the separation of heavy and precious metals from industrial effluents. For example, iron oxides have been used for extraction of environmental pollutants (Lin et al. 2010) and dyes from water solutions (Rocher et al. 2008).

There are numerous studies reporting covalent binding of very diverse molecules on carbon coatings through different strategies: a few examples include aryl species (Schumacher et al. 2012), norbornene tags (Schätz et al. 2010), positively charged polymer brushes (Zeltner et al. 2012), nitroxyl radicals (Schätz et al. 2008), and chloro, nitro, and amino groups (Grass et al. 2007). Physisorption of thin polymer layers on carbon shells of MNPs has also been reported (Fuhrer et al. 2010). Carbon-coated Fe_3O_4 MNPs have been modified with chitosan to extract polycyclic aromatic hydrocarbons (PAHs), perfluorinated compounds, and phthalate esters from water (Zhang et al. 2010).

Silanes are often used for stabilization and functionalization of MNPs, since they form a dense layer which can be covalently linked to metal oxide surfaces under mild conditions. In addition, they are commercially available with a wide range of functional end groups, allowing a versatile chemistry for further modification (De Palma et al. 2007). Recovery of metals and adsorption of different organic substances by silane-modified magnetic particles have been previously reported (Kraus et al. 2009; Wu and Xu 2005; Zhang et al. 2011), and MNPs have been synthesized with dual functional amino and thiol moieties for the recovery of Pb^{2+} and Mn^{2+} (Guo et al. 2010). In addition, magnetite nanoparticles modified with different silanes such as alkyl or aminopropyltriethoxy silanes have shown potential as immobilization media for biocatalysts (e.g., lipases) enabling efficient recovery and recycling of the catalysts (Kanimozhi and Perinbam 2013; Wang et al. 2012).

It was shown that polymer-modified carbon-coated cobalt nanoparticles (Co@C NPs) can be used for effective adsorption of gold from dilute water solutions (Schumacher et al. 2012; Rossier et al. 2010). In these works, however, some of the particles produced by flame-spray synthesis showed defects on the carbon surface, resulting in cobalt leakage and requiring separation of leaked cobalt before further processing steps (Schumacher et al. 2012).

In the present work, the carbon coating of magnetic cobalt nanoparticles was carried out by a hydrogen reduction method which has been scaled up in our facilities to a production range of about 2 kg per day (Hokkinen et al. 2014). The carbon shell of these cobalt nanoparticles fully prevented cobalt release into water at neutral pH, and contained oxidized moieties which allowed their facile surface functionalization with different organic alkoxysilanes, thus enabling a versatile surface chemistry for further modification. Finally, we show here that the Co@C NPs modified

with a silane containing a thiol group could achieve metal adsorption from both model aqueous gold solutions and thiocyanate-leached solutions prepared from crushed electronic circuit boards.

Beside the fact that their production process is very economical and scalable, the Co@C NPs used in this work are advantageous since each of their three components, i.e., magnetic core, protective shell, and functional groups, are all highly performing, yet are joined smoothly as one functional unit. The magnetic Co core has a high magnetic moment which leads to efficient separation of the particles. The carbon coating is very thin (about 2 nm) and therefore adds very little mass to the particles, while still protecting them to a large extent against oxidation and leakage even in mildly acidic solutions. Finally, the surface of the particles can be effectively modified, thanks to the presence of reactive oxidized functions, thus allowing in principle the introduction of specific functionalities in sight of sensing, catalytic, and separation applications.

Experimental section

Nanoparticle production

The particle production method is described in detail by Koskela et al. (2011). The synthesis of the nanoparticles has been performed using a single-piece quartz reactor. The precursor powder $CoCl_2$ was fed by a powder feeder to a heated evaporation column composed of porous alumina pellets kept at a temperature of 800 °C, which maximizes the evaporation area of the precursor. The evaporated precursor was carried along a nitrogen gas flow to the reaction zone, where hydrogen gas was fed to the metal chloride–nitrogen mixture at 950 °C.

The carbon coating on the cobalt nanoparticles was obtained by feeding an ethene–nitrogen mixture to the reaction zone together with hydrogen. The ethene (C_2H_4) content was 0.92 mol- % in the reaction zone, where it decomposed to methane (CH_4), ethane (C_2H_6), and carbon (C). The reaction was incomplete, and over 50 mol- % of the ethene remained unreacted. The metal surface catalyzes the decomposition reaction and the formation of the carbon layer, which suppresses further growth of the metal nanoparticles and controls the average diameter of their cores. The flow was then quenched with room temperature nitrogen gas, and Co@C NPs were collected on PTFE filter bags. The carbon-coating method is discussed in detail in Forsman et al. (2013), together with a full characterization of the particles including TEM and XRD analyses. The ethene degradation method has been proved in these prior experiments to produce a thin graphitic coating on the particles.

Before further use and functionalization, residual $CoCl_2$ was first repeatedly washed from the Co@C NPs with de-ionized water purged with nitrogen, and then dried under nitrogen gas flow at room temperature.

In order to verify the stability of the particles for storage and shipping and to investigate the possible release of Co, a series of tests were performed by leaving the Co@C NPs in an aqueous environment for variable amounts of time. The washed Co@C NPs were dispersed in 10 ml Milli-Q water purged with nitrogen. The release of cobalt ions from the purified Co@C NPs was studied for three different release times of 1, 7, and 35 days.

Surface functionalization of Co@C NPs

3-aminopropyltriethoxysilane (APTES) and 3-mercaptopropyltrimethoxysilane (MPTS) were used as modifying agents as described below.

For APTES modification, the effect of pre-treatment by UV/ozonation was also studied. 150 mg of Co@C MNPs was treated for 10 min in a UV/ozone chamber (ProCleaner Plus, BioForce Nanosciences) immediately before the functionalization with the silane. A 100-mg aliquot of pre-oxidized or non-pre-treated Co@C MNPs was dispersed into 10 ml of a 10 % (v/v) solution of APTES in ethanol and treated for 4 h in an ultrasonic bath, while keeping the temperature below 40 °C. After the sonication, the particles were washed twice with 5 ml of ethanol and then dried overnight in an oven at 50 °C. The same procedure was used to carry out MPTS modification, without any pre-oxidation and with 1-h reaction time.

Particle characterization

Scanning electron microscopy (SEM, Merlin® by Carl Zeiss NTS GmbH) was used to characterize the washed particulate materials for particle size, morphology, and elemental composition using an energy

dispersive X-ray detector (EDX) coupled to the SEM. The surface area of the particles was determined using the Brunauer–Emmett–Teller (BET, Micromeritics TriStar3000) gas sorption measurements method. For a more specific chemical composition study of the particle surface, high-resolution X-ray photoelectron spectroscopy (XPS, AXIS Ultra by Kratos) analysis was carried out using monochromatic Al Kα irradiation at 100 W. The data were analyzed with CasaXPS^{TM}. The cobalt concentration within the release test solutions after magnetic separation of Co@C NPs was determined by ion chromatography–mass spectroscopy (ICP-MS, Perkin Elmer NexION).

The quantity of free amino groups on the surface of APTES-modified Co@C NPs was determined with the ninhydrin assay, using glycin as a standard reference (Chen et al. 2009). The optical density was measured on a UV–Vis spectrometer (UV/VIS Shimadzu 2600) at 570 nm wavelength. The density of amino groups thus measured (120 nmol/mg of particles) was later used also as an approximate estimation of the surface density of thiol groups on MPTS-modified particles. Both APTES- and MPTS-modified samples were analyzed with SEM-EDX and XPS as well.

Metal adsorption experiments

Gold adsorption experiments in solution were performed with MPTS-modified particles, using both large (20:1) and small (3:1) molar excess of gold ions with respect to the estimated surface thiol groups. In the first test (large gold excess), 20.0 mg of MPTS-modified particles was incubated overnight with 10 ml of an aqueous solution containing 16.8 mg of $HAuCl_4$. In the second test (small gold excess), 20.0 mg of MPTS-modified particles was incubated with 2 ml of an aqueous solution containing 2.4 mg of $HAuCl_4$ for 3 h. In both cases, the samples were recovered by magnetic separation, washed three times with Milli-Q water, and dried overnight in an oven at 105 °C.

A leached thiocyanate solution obtained from crushed circuit boards was also used as a test sample for recovering metals with the MPTS-modified Co@C NPs. Leaching was carried out in a continuously stirred tank reactor using Fe^{3+} as an oxidation agent. The complex precursor was sodium thiocyanate, and the pH was brought to a value of 2–3 with sulfuric acid (Kähäri 2013). A 100-mg aliquot of MPTS-modified Co@C NPs was kept in 1.5 ml of the thiocyanate-leached solution for 3 h. The solution was analyzed with ICP-MS before and after incubation and magnetic separation of the particles. The particles were washed three times with ethanol and dried overnight in an oven at 50 °C before SEM-EDX analyses.

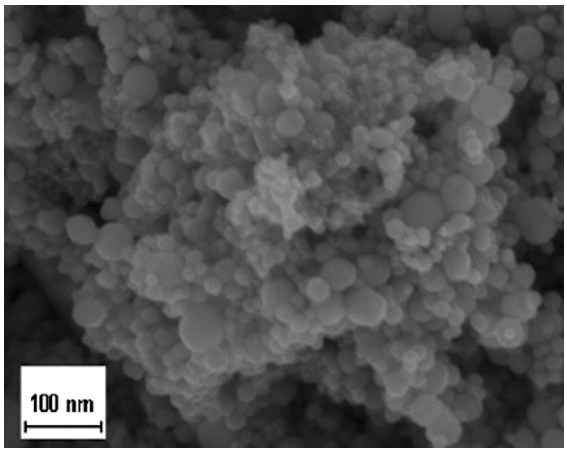

Fig. 1 SEM micrograph of the washed Co@C NPs (*scale bar* 100 nm)

Results and discussion

Preparation of the magnetic particles

The structure and composition of the Co@C NPs prepared by hydrogen reduction synthesis method were first studied by electron microscopy. The SEM image of the Co@C NPs after washing shown in Fig. 1 displays particles with an average primary diameter of 29 ± 9 nm. The specific surface area of the particles, as measured by the BET analysis, was 25.5 m^2/g. This result is in good agreement with the theoretical value of 23.2 m^2/g, calculated from size distribution data gathered from SEM images for pure Co@C NPs with average diameter of 29 nm, confirming the accessibility of the particle surface even in a dry state.

The SEM-EDX maps shown in Fig. 2b–c, together with the XPS data (Table 1), demonstrate the presence of both oxygen and carbon on the particle surface. The high-resolution XPS spectrum of Co 2p (Fig. 3a) indicates that most of the oxygen came from Co oxides, as testified by the presence of a broad Co 2p component at 781.9 ± 0.3 eV as opposed to the sharp metallic Co 2p component at 778.9 ± 0.2 eV. It should, however, be noted that the ratio of metallic

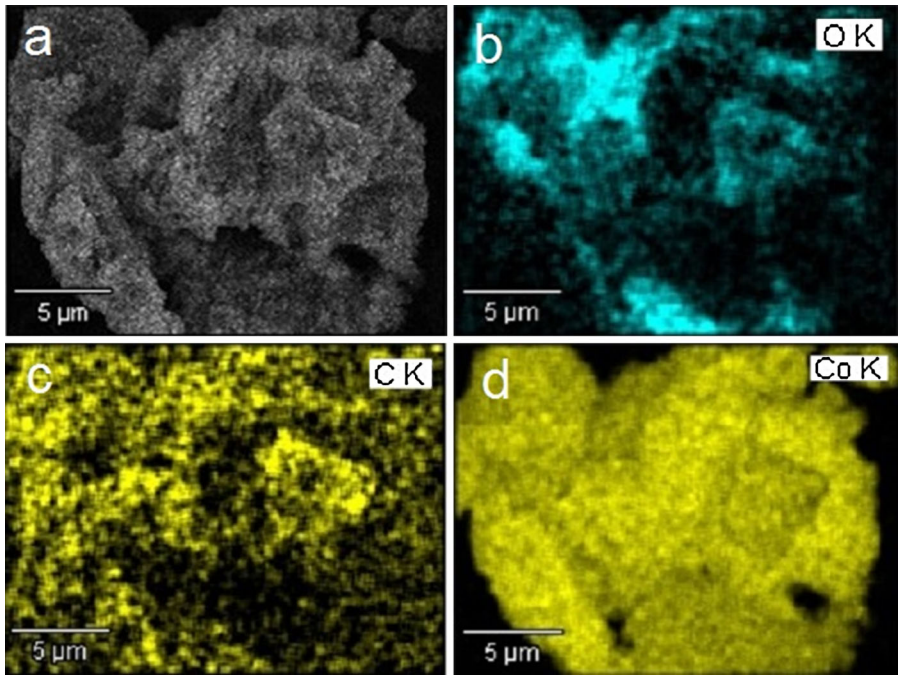

Fig. 2 SEM-EDX **a** base image, and elemental mapping for **b** oxygen, **c** carbon, and **d** cobalt content of the surface of the washed Co@C NPs (*scale bar* 5 µm)

Table 1 Atomic concentrations from parallel XPS analyses for washed, APTES- and MPTS-modified Co + C NPs. (I) and (II) denote different areas of the samples

	Atomic concentrations (%)							
	O 1 s	C 1 s	Co 2p	N 1 s	Si 2p	S 2p	Zn 2p	Cl 2p
Co + C NPs (I)	33.1	32.2	31.7				1.8	1.1
Co + C NPs (II)	28.9	36.4	32.2				1.7	0.8
Co + C NPs APTES (I)	16.7	46.6	31.1	3.0	2.6			
Co + C NPs APTES (II)	16.5	47.3	31.8	2.3	2.2			
Co + C NPs MPTS (I)	24.9	53.4	8.0		7.8	5.8		
Co + C NPs MPTS (II)	25.6	53.0	7.7		8.0	5.7		

and oxidized cobalt compounds in the Co 2p spectrum showed significant variability between different measurement spots, with the highest cobalt oxide content observed in the case shown in Fig. 3a. Together the XPS and SEM results suggest a somewhat uneven oxidation of the washed particles. A relevant portion of the oxygen content was, however, associated also with the oxidation of the carbon shell. In fact, fitting of the C 1 s peak in Fig. 3b revealed the presence of several carbon components assignable to different oxidation states, i.e., C–C (67.2 %), C–O (17.4 %), C = O (5.6 %), and COO (9.7 %). The presence of these components indicates that the native carbon shell covering the MNPs features a number of oxidized sites, likely including C–OH groups which may be exploited for reaction with alkoxysilanes.

In order to verify the efficiency of the carbon shell to prevent cobalt leakage in solution under conditions relevant for particle storage and shipping, ICP-MS tests were performed to assess the Co content in Milli-Q water samples incubated with the Co@C NPs for variable times (1, 7, and 35 days). The maximum average value obtained in the series corresponded to 0.72 wt% of the Co@C NPs used for the incubation (Table 2). This small value is probably related to the presence of traces of residual Co@C NPs not collected during the magnetic separation step, or to experimental error in the ICP analysis method, rather than to leakage of Co ions in solution or dissolution of cobalt oxide, which is not expected to occur under the neutral or

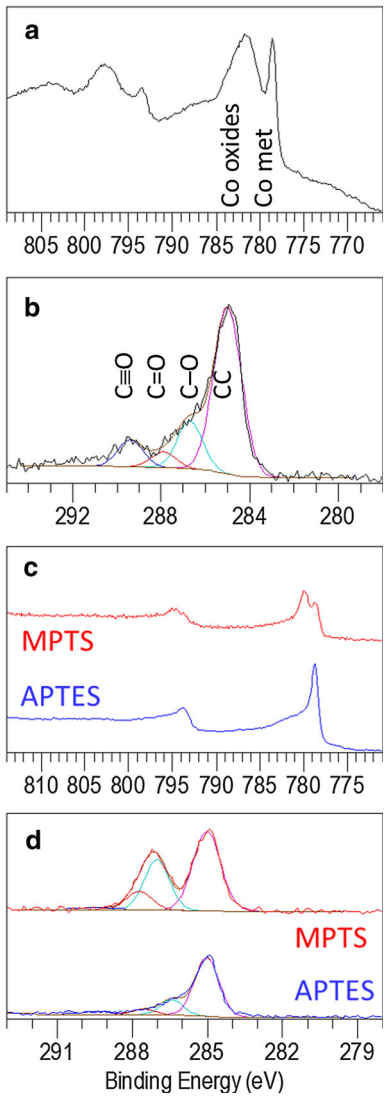

Fig. 3 XPS high-resolution data on the washed Co@C NPs for **a** Co 2p and **b** C 1 s regions, and on the silane-treated NPs for **c** Co 2p and **d** C 1 s regions

slightly acidic conditions expected for Milli-Q water, where the pH typically drops to about 5.5 over time due to CO_2 absorption. It appears, therefore, reasonable to conclude that the graphitic carbon shell does effectively protect the cobalt nanoparticles under these conditions.

Surface functionalization of the magnetic nanoparticles

Achieving control over the surface chemistry of the MNPs holds the potential to perform further modification to enable a great number of different applications, for example in the fields of separation, imaging, catalysis, or biomedical devices. Since the carbon shell of the Co@C NPs showed to possess a number of potentially reactive oxidized sites, we introduced amino and thiol groups on the surface of the particles by treatment with APTES and MPTS. The functionalization is expected to occur by means of a condensation reaction between the hydroxyl groups present on the oxidized carbon shell and the silanols generated by hydrolysis of the alkoxysilanes. Therefore, we investigated also the possibility to increase the reactivity of the particle surface through a mild oxidation pre-treatment performed by ozonation, which may generate additional oxidized moieties including hydroxyl groups. The SEM images revealed that the size and morphology of the APTES-modified Co@C NPs remained quite unchanged both for the non-pre-treated and the ozone-pre-treated particles (Fig. S1 in Supporting Information), which displayed sizes of ca. 30 nm. The morphology of these particles was not significantly affected either by the pre-oxidation or by the silane treatment, indicating that the carbon shell could withstand the operating conditions and that the deposited APTES layer was very thin, possibly monomolecular. The successful modification of the nanoparticles with APTES was demonstrated by EDX analyses, which showed a rather homogeneous distribution of the silane over the surface of the particles (Fig. 4 and S2 in Supporting Information). The EDX detected rather similar low amounts of Si within the two samples (around 0.7 wt% for non-pre-treated, and 0.9 wt% for pre-treated particles), confirming the hypothesis of a very thin silane layer on the particle surface and suggesting that although the

Table 2 Cobalt content in release test solutions after specific release times, as measured by ICP-MS

Co + C powder (mg)	Release time (days)	Residual Co in solution (mg/l)	Co(solution)/ Co(solid) (average wt%)
2.0	1	1.7	0.72
1.9	1	1.4	
1.9	1	1.1	
2.1	7	1.0	0.6
1.9	7	1.3	
2.0	7	1.3	
1.9	35	1.1	0.61
2.2	35	1.4	
0 (blank)	–	0.6	–

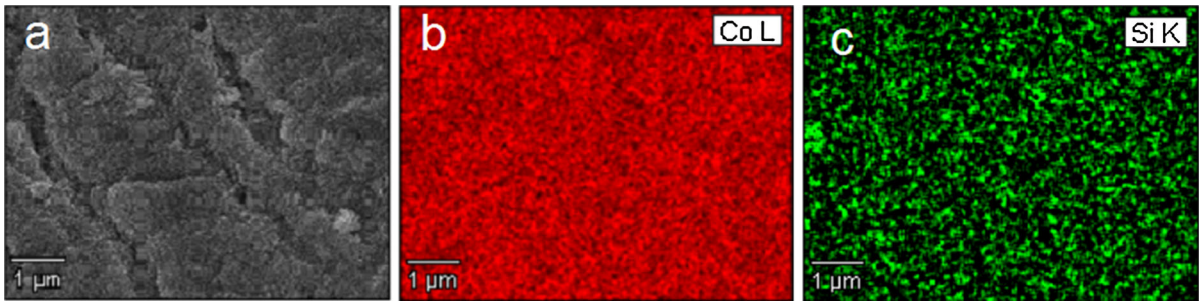

Fig. 4 SEM **a** image and EDX elemental mapping of **b** cobalt and **c** silicon for APTES-modified, non-pre-treated Co@C NPs (*scale bar* 1 µm)

pre-oxidation seems to slightly improve the particle reactivity toward surface modification, it is possible to obtain satisfactory results even without preliminary ozonation. Therefore, all subsequent work was carried out without this pre-treatment.

Rather similar results were obtained for the MPTS modification, showing that the Si and S distribution on the surface of the particles was quite homogeneous (Fig. S3 in Supporting Information), and that also in this case, a thin silane layer was deposited.

The density of the accessible surface amino groups on APTES-modified Co@C NPs was determined quantitatively by the ninhydrin assay, which yielded a coverage of 120 nmol/mg. XPS analysis further confirmed the formation of the silane layers on the surface of the nanoparticles. Nitrogen and sulfur from amino and thiol groups were detected clearly, as shown in Table 1. One apparent difference between the APTES- and MPTS-modified samples lies in the fact that the latter featured significantly higher carbon, oxygen, and silicon content, which can be associated with a slightly thicker silane layer, as well as with an incomplete hydrolysis of the methoxy groups in the MPTS-modified sample. This is consistent with the presence of a particularly strong C 1 s component at 287.0 ± 0.2 eV (Fig. 3d), and with the shorter reaction time employed during the functionalization of Co@C NPs with MPTS, when compared to APTES.

It should be noted also that in the MPTS-functionalized samples, a sharp feature was observed at 780.0 ± 0.2 eV in the Co 2p high-resolution peak (Fig. 3c). This appears to be associated with cobalt-sulfur interactions rather than with the presence of cobalt oxide, since the same feature was not observed in the APTES-modified sample. The onset of such a signal likely arises from traces of Co compounds present as impurities in the sample.

The results, here, described show that it was possible to modify the surface chemistry of the Co@C NPs through simple silane coupling under mild preparation conditions. The functional groups introduced can be exploited for further modification; the particles modified with amino groups are promising intermediates in this sense, while the MPTS-modified Co@C NPs could be used either for further modification or even as such for metal adsorption, with gold being an ideal candidate.

Metal adsorption tests

We verified the ability of both unmodified and MPTS-modified Co@C NPs to collect gold from aqueous solutions containing either large or small excess of $HAuCl_4$ with respect to the thiol groups coverage. The density of exposed thiol groups was assumed to be of the same order as the surface coverage of amino groups derived for APTES-modified particles. In all cases, the solutions became completely discolored, suggesting that all the gold was extracted from the aqueous phase; this was not observed in control experiments performed in the absence of any magnetic particles. When a ca. 20-fold molar excess of gold was used, the EDX elemental mapping showed that gold was indeed adsorbed on both the unmodified and the MPTS-modified Co@C NPs (Fig. 5), but in a rather inhomogeneous manner. The high-resolution SEM images (Fig. 5c, f) showed the presence of gold crystallites, assembled into structures up to 2 µm in size, which were rather similar in both samples. It appears that the nanoparticles initiate the nucleation of gold which assembles into crystallites when present in

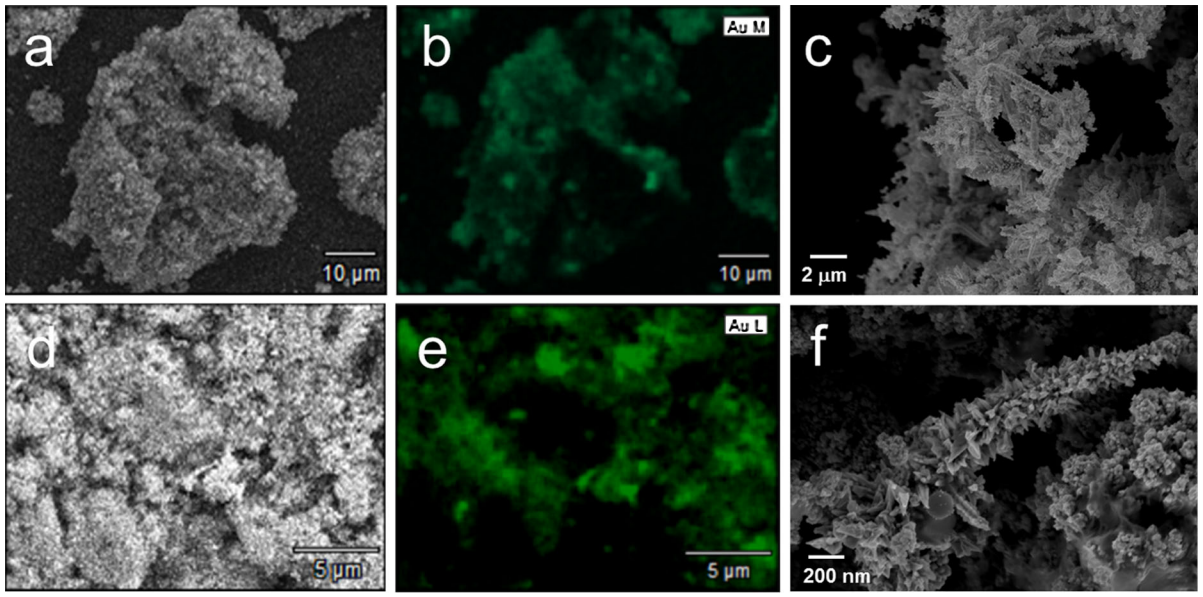

Fig. 5 SEM-EDX images and Au mapping (**b**, **e**) of non-modified Co@C NPs (**a**, **b**, **c**; *scale bars*: *a*, $b = 10$ µm, $c = 2$ µm) and of MPTS-modified Co@C NPs (**d**, **e**, **f**; *scale bars*: *d*, $e = 5$ µm, $f = 200$ nm) incubated with a 20-fold excess of gold

high quantities. The similarity of the results observed for non-modified and MPTS-modified MNPs may be due to the presence of oxidized moieties on the carbon shell of pristine particles.

However, differences in behavior were observed when a significantly smaller excess of gold (ca. 3-fold) was used. In this case, the gold was adsorbed more homogeneously on the surface of the MPTS-modified Co@C NPs than on the non-modified particles, as testified by the presence of fewer high gold concentration regions in the SEM-EDX images (Fig. 6). The high-resolution SEM images (Fig. 6c, f) showed fewer large gold crystals on the silane-modified particles, suggesting that they were covered with a thin and homogeneous layer of adsorbed gold. This result is likely due to a higher affinity for gold of the thiol groups when compared to the oxidized carbon shell of the pristine particles; so that on MPTS-modified Co@C NPs, the binding of gold to free thiol sites can compete more efficiently with the growth of crystallites on sites where gold is already adsorbed.

The metal adsorption capabilities of the MPTS-modified Co@C NPs were tested also by incubation in a thiocyanate-leached solution obtained from printed circuit boards, and by analyzing the metal contents of the solution by ICP-MS before and after incubation (Table 3). The amount of dissolved cobalt increased significantly, corresponding roughly to 4 wt% of the particles used during the incubation. This seems to indicate that some Co leakage occurred under the acidic conditions of the test (pH 2), although the particles could still be magnetically separated from the solution and their SEM images did not show particular signs of damage (Fig. S4 in Supporting Information). This small Co leakage may be due to the presence of a minimal portion of particles with an imperfect carbon coating, making them more susceptible to oxidation and dissolution under these conditions; in any case, overall, this result confirms the good efficiency of the carbon shell in protecting the vast majority of the particles even in significantly acidic environments.

When comparing the metal concentrations before and after incubation, the ICP-MS analyses indicated that the thiolated MPTS-modified Co@C NPs adsorbed most effectively Au and Cu, as expected. Moderate adsorption of Sn and Al occurred, while little to no affinity was observed toward Mn and Ni. The sample solution contained high amounts of Fe, of which 1–2 % was apparently adsorbed on the NPs. Although the values for iron are affected by a high experimental uncertainty, this element could be clearly observed by SEM-EDX measurements on the recovered MPTS-

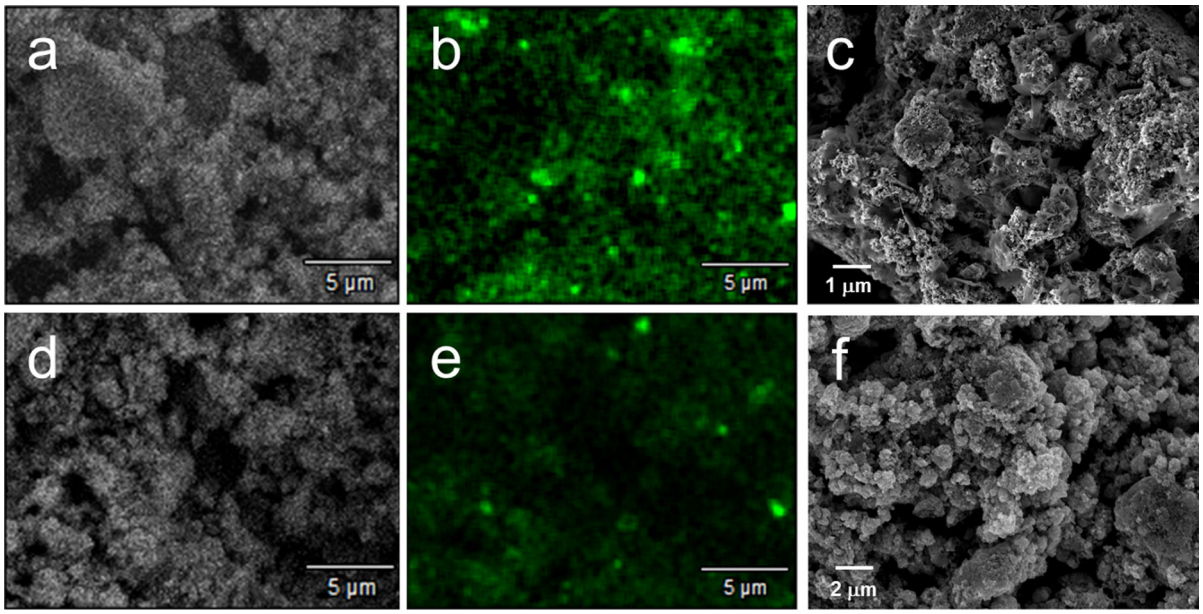

Fig. 6 SEM-EDX images and Au mapping (**b**, **e**) of non-modified Co@C NPs (**a**, **b**, **c**; *scale bars*: *a*, *b* = 5 μm, *c* = 1 μm) and of MPTS-modified Co@C NPs (**d**, **e**, **f**; *scale bars*: *d*, *e* = 5 μm, *f* = 2 μm) incubated with a 3-fold excess of gold

Table 3 Metal concentrations in leached thiocyanate solutions before and after incubation with MPTS-modified Co + C NPs, as measured by ICP-MS

	Al	Au	Co	Cu	Fe	Mn	Ni	Si	Sn
Before incubation (mg/ml)	23	16	14	19	8,700	30	1,700	14	230
After incubation, sample I (mg/ml)	20	3.8	2,800	1.9	8,600	30	1,700	15	110
After incubation, sample II (mg/ml)	12	1.8	3,100	0.5	8,600	29	1,700	15	38
Measure uncertainty (%)	25	30	15	20	20	20	25	25	20
Adsorbed metal[a] (μg)	10	20	n/a	27	150	1	0	n/a	234

[a] Amount of metal adsorbed by 100 mg of particles upon incubation with 1.5 ml of leached solution, as estimated from the metal concentrations in solution before and after incubation

modified Co@C NPs, along with most of the other highly adsorbing metals (Fig. S5 in Supporting Information). The thiol group binds strongly to metals like gold or mercury, but as a soft ligand it might also form complexes with a variety of other metals, like nickel, tin, manganese, or iron, with the stability of the metal-thiol complexes following that of the corresponding metal sulfides. Therefore, the binding of gold is rather strong but not fully selective, and smaller portions of other metals may also be adsorbed by complex formation. However, in the present case, the moderate adsorption of metals other than gold and copper can also be due to exposed silanol groups left by a non-quantitative condensation of the hydrolyzed MPTS, and potentially also by the presence of small areas of the oxidized carbon shell of the nanoparticles remained accessible even after silane functionalization.

The EDX analyses indicated that metal adsorption onto the particles occurred rather homogeneously. The degree of selectivity of this system is expectedly limited, and could in principle be increased by further functionalization with other chemical functions or with biomolecules able to achieve more selective metal binding.

Conclusions

We have reported the preparation of magnetic cobalt nanoparticles protected with a thin carbon shell by means of an easily scalable method. The carbonaceous

protective layer effectively prevents cobalt leakage in neutral aqueous solutions, and features oxidized chemical sites which enable the modification of the particle surface chemistry by silane coupling under mild conditions. This versatile method could be used to introduce different functionalities on the surface of the Co@C NPs with a simple and relatively inexpensive procedure, potentially providing a great number of applications e.g. in the fields of separation, catalysis, and sensing. The APTES-modified Co@C NPs, in particular, have a great potential for further modification, including introduction of (bio)molecules for highly specific binding or detection of target compounds. Finally, we showed that both pristine and MPTS-modified particles can be used already as such for the adsorption of metals from solution, even exceeding their theoretical maximum binding capacity in the case of gold adsorption. The MPTS-modified particles, in particular, could be used to adsorb gold as a homogeneous thin layer under moderate metal excess conditions, and allowed successful adsorption of several different metals from a thiocyanate-leached solution obtained from crushed printed circuit boards.

The development of MNP-based applications has been suffering from the lack of affordable metallic nanomaterials. To meet this challenge, we have recently developed a large scale pilot reactor based on hydrogen reduction synthesis process, which is expected to allow the convenient synthesis of nanomaterials with high production rates and week-long continuous operation in the future. With such synthesis process, the price of the carbon-coated nanomagnets is expected to be sufficiently low e.g., for separation of precious metals, thereby making the overall process more economically viable; experiments in this sense are currently being carried out in our laboratories and will be the object of a future communication.

Acknowledgments The authors are grateful to Mr. Raoul Järvinen for his production facility design and construction work, and to Dr. J.M. Campbell for performing the XPS experiments. Also Mr. Jarno Mäkinen is thanked for providing the thiocyanate-leached sample from crushed circuit boards. Financial support from VTT Technical Research Centre of Finland under the project AERTO is gratefully acknowledged.

References

Baldelli Bombelli F, Webster CA, Moncrieff M, Sherwood V (2014) The scope of nanoparticle therapies for future metastatic melanoma treatment. Lancet Oncol 15:e22–e32

Behrens S (2011) Preparation of functional magnetic nanocomposites and hybrid materials: recent progress and future directions. Nanoscale 3:877–892

Chen S, Hayakawa S, Shirosaki Y, Fujii E, Kawabata K, Tsuru K, Osaka A (2009) Sol-gel synthesis and microstructure analysis of amino-modified hybrid silica nanoparticles from aminopropyltriethoxysilane and tetraethoxysilane. J Am Ceram Soc 92:2074–2082

De Palma R, Peeters S, Van Bael MJ, Van den Rul H, Bonroy K, Laureyn W, Mullens J, Borghs G, Maes G (2007) Silane ligand exchange to make hydrophobic superparamagnetic nanoparticles water-dispersible. Chem Mater 19:1821–1831

Forsman J, Koskela P, Auvinen A, Tapper U, van Dijken S, Jokiniemi J (2013) In-situ coated nanomagnets. Powder Technol 233:15–21

Fuhrer R, Herrmann IK, Athanassiou EK, Grass RN, Stark WJ (2010) Immobilized β-cyclodextrin on surface-modified carbon-coated cobalt nanomagnets: reversible organic contaminant adsorption and enrichment from water. Langmuir 27:1924–1929

Grass RN, Athanassiou EK, Stark WJ (2007) Covalently functionalized cobalt nanoparticles as a platform for magnetic separations in organic synthesis. Angew Chem Int Ed 46:4909–4912

Guo Q, Xue Y, Guo J, Yan G, Li L (2010) Magnetic nanoparticles derivatized with both functional moieties for the recovery of heavy metal ions in environmental water. Adv Mater Res 129–131:617–620

Hokkinen J, Tapper U, Mattila P, Auvinen A, Jokiniemi J (2014) Pilot scale production of metal nano powders from chloride precursors. Poster presentation, Conference on Aerosol Technology 2014, 16–18 June, Karlsruhe, Germany

Jedlovszky-Hajdú A, Baldelli Bombelli F, Monopoli MP, Tombácz E, Dawson KA (2012) Surface coatings shape the protein corona of SPIONs with relevance to their application in vivo. Langmuir 28:14983–14991

Kähäri M (2013) Dissolution and Recovery of Gold with Cyanide Replacing Hydrometallurgical Processes. Master thesis dissertation, Aalto University

Kanimozhi S, Perinbam K (2013) Synthesis of amino-silane modified superparamagnetic Fe_3O_4 nanoparticles and its application in immobilization of lipase from *Pseudomonas fluorescens* Lp1. Mater Res Bull 48:1830–1836

Koskela P, Teirikangas M, Alastalo A, Forsman J, Juuti J, Tapper U, Auvinen A, Seppä H, Jantunen H, Jokiniemi J (2011) Synthesis of cobalt nanoparticles to enhance magnetic permeability of metal–polymer composites. Adv Powder Technol 22:649–656

Kraus A, Jainae K, Unob F, Sukpirom N (2009) Synthesis of MPTS-modified cobalt ferrite nanoparticles and their adsorption properties in relation to Au(III). J Colloid Interface Sci 338:359–365

Lin J, Wu Z, Tseng W (2010) Extraction of environmental pollutants using magnetic nanomaterials. Anal Methods 2:1874–1879

Liu Y, Su G, Zhang B, Jiang G, Yan B (2011) Nanoparticle-based strategies for detection and remediation of environmental pollutants. Analyst 136:872–877

Rocher V, Siaugue J, Cabuil V, Bee A (2008) Removal of organic dyes by magnetic alginate beads. Water Res 42:1290–1298

Rossier M, Koehler FM, Athanassiou EK, Grass RN, Waelle M, Birbaum K, Gunther D, Stark WJ (2010) Energy-efficient noble metal recovery by the use of acid-stable nanomagnets. Ind Eng Chem Res 49:9355–9362

Schätz A, Grass RN, Stark WJ, Reiser O (2008) TEMPO supported on magnetic C/Co-nanoparticles: a highly active and recyclable organocatalyst. Chem Eur J 14:8262–8266

Schätz A, Long TR, Grass RN, Stark WJ, Hanson PR, Reiser O (2010) Immobilization on a nanomagnetic Co/C surface using ROM polymerization: generation of a hybrid material as support for a recyclable palladium catalyst. Adv Funct Mater 20:4323–4328

Schumacher CM, Grass RN, Rossier M, Athanassiou EK, Stark WJ (2012) Physical defect formation in few layer graphene-like carbon on metals: influence of temperature, acidity, and chemical functionalization. Langmuir 28:4565–4572

Seo WS, Lee JH, Sun X, Suzuki Y, Mann D, Liu Z, Terashima M, Yang PC, Mcconnell MV, Nishimura DG, Dai H (2006) FeCo/graphitic-shell nanocrystals as advanced magnetic-resonance-imaging and near-infrared agents. Nat Mater 5:971–976

Song Y, Wang R, Rong R, Ding J, Liu J, Li R, Liu Z, Li H, Wang X, Zhang J, Fang J (2011) Synthesis of well-dispersed aqueous-phase magnetite nanoparticles and their metabolism as an MRI contrast agent for the reticuloendothelial system. Eur J Inorg Chem 22:3303–3313

Song Y, Ding J, Wang Y (2012) Shell-dependent evolution of optical and magnetic properties of Co@Au core—shell nanoparticles. J Phys Chem C 116:11343–11350

Song Y, Ji S, Song YJ, Li R, Ding J, Shen X, Wang R, Xu R, Gu X (2013) In Situ redox microfluidic synthesis of core—shell nanoparticles and their long-term stability. J Phys Chem C 117:17274–17284

Sun Y, Duan L, Guo Z, DuanMu Y, Ma M, Zhang Y, Ning G (2005) An improved way to prepare superparamagnetic magnetite-silica core-shell nanoparticles for possible biological application. J Magn Magn Mater 285:65–70

Villani M, Rimoldi T, Calestani D, Lazzarini L, Chiesi V, Casoli F, Albertini F, Zappettini A (2013) Composite multifunctional nanostructures based on ZnO tetrapods and superparamagnetic Fe_3O_4 nanoparticles. Nanotechnology 24(9):135601

Wang J, Meng G, Tao K, Feng M, Zhao X, Li Z, Xu H, Xia D, Lu JR (2012) Immobilization of lipases on alkyl silane modified magnetic nanoparticles: effect of alkyl chain length on enzyme activity. PLoS One 7(8):e43478

Wu PG, Xu ZH (2005) Silanation of nanostructured mesoporous magnetic particles for heavy metal recovery. Ind Eng Chem Res 44:816–824

Yan K, Li P, Zhu H, Zhou Y, Ding J, Shen J, Li Z, Xu Z, Chu PK (2013) Recent advances in multifunctional magnetic nanoparticles and applications to biomedical diagnosis and treatment. RSC Adv 3:10598–10618

Zeltner M, Grass RN, Schaetz A, Bubenhofer SB, Luechinger NA, Stark WJ (2012) Stable dispersions of ferromagnetic carbon-coated metal nanoparticles: preparation via surface initiated atom transfer radical polymerization. J Mater Chem 22:12064–12071

Zhang XL, Niu HY, Zhang SX, Cai YQ (2010) Preparation of a chitosan-coated C_{18}-functionalized magnetite nanoparticle sorbent for extraction of phthalate ester compounds from environmental water samples. Anal Bioanal Chem 397: 791–798

Zhang X, Niu H, Yan J, Cai Y (2011) Immobilizing silver nanoparticles onto the surface of magnetic silica composite to prepare magnetic disinfectant with enhanced stability and antibacterial activity. Colloids Surf A 375:186–192

Zhang L, Dong W, Sun H (2013) Multifunctional superparamagnetic iron oxide nanoparticles: design, synthesis and biomedical photonic applications. Nanoscale 5:7664–7684

Zhu Y, Stubbs LP, Ho F, Liu R, Ship CP, Maguire J, Hosmane N (2010) Magnetic nanocomposites: a new perspective in catalysis. ChemCatChem 2:365–374